Synchronous Radiocarbon and Climate Shifts During the Last Deglaciation

Konrad A. Hughen, *et al.*

Science **290**, 1951 (2000);
DOI: 10.1126/science.290.5498.1951

24. N. J. Maloney, *Bol. Inst. Oceanogr. Univ. Oriente* **4**, 246 (1965).
25. T. Clayton, R. B. Pearce, L. C. Peterson, *Mar. Geol.* **161**, 191 (1999).
26. C. Schubert, *Interciencia* **13**, 128 (1988).
27. S. W. Hostetler, P. U. Clark, P. J. Bartlein, A. C. Mix, N. J. Pisias, *J. Geophys. Res.* **104**, 3947 (1999).
28. H. W. Arz, J. Pätzold, G. Wefer, *Quat. Res.* **50**, 157 (1998).
29. T. F. Stocker, D. G. Wright, *Nature* **351**, 729 (1991).
30. F. Zaucker, T. F. Stocker, W. S. Broecker, *J. Geophys. Res.* **99**, 12443 (1994).
31. P. K. Weyl, *Meteorol. Monogr.* **8**, 37 (1968).
32. A. V. Fedorov, S. G. Philander, *Science* **288**, 1997 (2000).
33. M. Cane , A. C. Clement, in (*2*), pp. 373–383.

34. This research was supported by the U.S. NSF (Division of Ocean Sciences) and the Deutsche Forschungsgemeinschaft. We thank A. Clement and C. Rooth for valuable discussion and J. Kennett and two anonymous referees for their thorough reviews. This work was made possible by the ODP and the efforts of the scientific party and crew of ODP Leg 165. This is a contribution from the Rosenstiel School of Marine and Atmospheric Science, University of Miami.

14 August 2000; accepted 9 November 2000

Synchronous Radiocarbon and Climate Shifts During the Last Deglaciation

Konrad A. Hughen,[1]* John R. Southon,[2] Scott J. Lehman,[3] Jonathan T. Overpeck[4]

Radiocarbon data from the Cariaco Basin provide calibration of the carbon-14 time scale across the period of deglaciation (15,000 to 10,000 years ago) with resolution available previously only from Holocene tree rings. Reconstructed changes in atmospheric carbon-14 are larger than previously thought, with the largest change occurring simultaneously with the sudden climatic cooling of the Younger Dryas event. Carbon-14 and published beryllium-10 data together suggest that concurrent climate and carbon-14 changes were predominantly the result of abrupt shifts in deep ocean ventilation.

Efforts to calibrate the radiocarbon time scale and to quantify the record of changes in past atmospheric ^{14}C concentration [Δ^{14}C, reported as per mil (‰) deviations from the preindustrial value] rely primarily on ^{14}C measurements on tree-ring dated wood (*1*, *2*). However, these dendrochronological records extend back only to ~11,900 calendar years before present (11.9 cal kyr B.P.) and do not provide calibration during most of the large, abrupt climate changes of the last deglaciation, including the Younger Dryas cold reversal. Paired U/Th-^{14}C dates from corals have been used to extend ^{14}C calibration back in time beyond that determinable by tree rings (*3*–*6*), revealing elevated Δ^{14}C during the Younger Dryas period. However, available ^{14}C calibration data from corals provide limited temporal resolution and do not constrain the decade-century scale details of past ^{14}C variation. Recently reported results (*7*) documenting abrupt changes in Δ^{14}C and climate during the onset of the Younger Dryas are consistent with the hypothesis that a shutdown of deep ocean ventilation caused shifts in both ^{14}C and climate (*7*–*11*). However, those data are not of high enough resolution to conclusively determine the timing of the Δ^{14}C shift relative to the Younger Dryas onset, leading to speculation that the Δ^{14}C changes were caused by another mechanism (e.g., solar variability) (*12*). Here we present ^{14}C data from Cariaco Basin core PL07-58PC (hereafter 58PC), providing 10- to 15-year resolution through most of deglaciation. The new calibration data demonstrate conclusively that Δ^{14}C changes were synchronous with climate shifts during the Younger Dryas. Calculated Δ^{14}C is strongly correlated to climate proxy data throughout early deglaciation ($r = 0.81$). Comparing Δ^{14}C and ^{10}Be records leads us to conclude that ocean circulation changes, not solar variability, must be the primary mechanism for both ^{14}C and climate changes during the Younger Dryas.

Cariaco Basin core 58PC (10°40.60′N, 64°57.70′W; 820 m depth) has an average sedimentation rate (70 cm/kyr) more than 25% higher than core 56PC (10°41.22′N, 64°58.07′W; 810 m depth) (*13, 14*), and shares similar hydrographic conditions. Restricted deep circulation and high surface productivity in the Cariaco Basin off the coast of Venezuela create an anoxic water column below 300 m. The climatic cycle of a dry, windy season with coastal upwelling, followed by a nonwindy, rainy season, results in distinctly laminated sediment couplets of light-colored, organic-rich plankton tests and dark-colored mineral grains from local river runoff (*13*). It has been demonstrated previously that the laminae couplets are annually deposited varves and that light laminae thickness, sediment reflectance (gray scale), and abundance of the foraminifer *Globigerina bulloides* are all sensitive proxies for surface productivity, upwelling, and trade wind strength (*14*, *15*). Nearly identical patterns, timing, and duration of abrupt changes in Cariaco Basin upwelling compared with surface temperatures in the high-latitude North Atlantic region at 1- to 10-year resolution during the past 110 years and the last deglaciation (*7*, *14*, *15*) provide evidence that rapid climate shifts in the two regions were synchronous. A likely mechanism for this linkage is the response of North Atlantic trade winds to the equator-pole temperature gradient forced by changes in high-latitude North Atlantic temperature (*16*).

The hydrography of the Cariaco Basin provides excellent conditions for ^{14}C dating (*17*). The shallow sills (146 m depth) constrain water entering the basin to the surface layer, well equilibrated with atmospheric CO_2. Despite anoxic conditions, the deep waters of the Cariaco Basin have a brief residence time, as little as 100 years (*17*). Two radiocarbon dates on *G. bulloides* of known recent calendar age gave the same surface water-atmospheric ^{14}C difference (reservoir age) as the open Atlantic Ocean (*7*). Good agreement during the early Holocene and Younger Dryas between Cariaco Basin and terrestrial ^{14}C dates, including German pines and plant macrofossils from lake sediments (*1*, *9*, *11*, *18*) (Fig. 1), suggests that Cariaco Basin reservoir age does not change measurably as a response to increased local upwelling (i.e., during the Younger Dryas) (*19*). Planktonic foraminiferal abundance permits continuous sampling at 1.5-cm increments, providing 10- to 15-calendar-year resolution throughout most of deglaciation.

For this work, the varve chronology is largely the same as that used for core 56PC (*7*). Varves have been re-counted during periods of particular importance, such as the overlap with tree rings and the onset of the Younger Dryas, as well as the deepest, oldest laminations that are less distinct. The floating Cariaco Basin varve chronology was anchored to the German pine dendrochronology by wiggle-matching ^{14}C variations in both curves (Fig. 1). The correla-

[1]Department of Marine Chemistry and Geochemistry, Woods Hole Oceanographic Institution, Woods Hole, MA 02543, USA. [2]Center for Accelerator Mass Spectrometry, Lawrence Livermore National Laboratory, Livermore, CA 94551, USA. [3]Institute of Arctic and Alpine Research and Department of Geological Sciences, University of Colorado, Boulder, CO 80309, USA. [4]Institute for the Study of Planet Earth and Department of Geosciences, University of Arizona, Tucson, AZ 85721, USA.

*To whom correspondence should be addressed. E-mail: khughen@whoi.edu

tion between the two time series is excellent, $r = 0.989$ (Fig. 1, inset), anchoring the Cariaco Basin floating chronology to an absolute calendar time scale (*20*). Independent confirmation for this age match is provided by the close agreement for the timing of the Younger Dryas termination recorded by tree rings (11,570 cal yr B.P.) and Cariaco Basin gray scale (11,565 cal yr B.P., ±10 years relative to tree rings) (*20*).

The anchored Cariaco Basin varve chronology provides radiocarbon calibration at high resolution from ~14.8 to 10.5 cal kyr B.P. (Fig. 2) (*21*). The abrupt beginning and end of the large drop in ^{14}C age during the Younger Dryas onset are shown to be sharp changes in slope rather than gradual transitions. A ^{14}C plateau can be discerned at 11.7 to 11.8 ^{14}C kyr B.P., lasting about 250 calendar years. The oldest part of the record is characterized by another plateau at 12.5 ^{14}C kyr B.P., extending beyond (*18*) the Glacial/Bølling boundary where the Cariaco Basin laminations begin. A decrease in ^{14}C age at the Younger Dryas onset of the same amplitude as core 58PC is also seen in coral and Lake Suigetsu data (Fig. 2). In addition, some of the same fine structure during the Younger Dryas in core 58PC is also reported in corals from Vanuatu (*6*), although there is a slight offset in the steep ^{14}C decline around 12.4 cal kyr B.P. (Fig. 2). The similar trends suggest this offset may result from reservoir age differences between the Atlantic and Pacific Oceans.

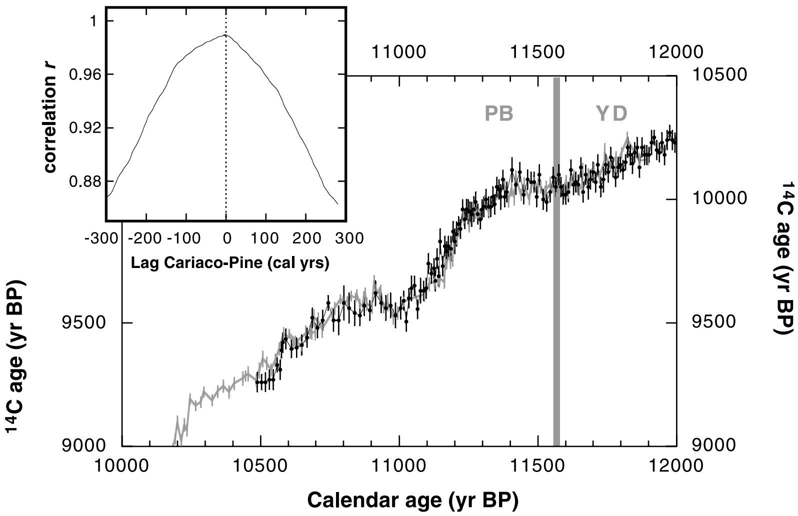

Fig. 1. Correlation of variations in ^{14}C compared with calendar age for Cariaco Basin core PL07-58PC and German pines (*1*). Thick gray line, German pine data set; thin black line and solid circles, Cariaco Basin data. The German pine data set has been revised recently with the addition of 40 years at 11,330 cal yr B.P. (*39*). The Cariaco and pine ^{14}C data sets were interpolated and resampled at even 5-year increments and were correlated within a moving 1370-year window. The window was shifted in 5-year steps through time lags of ±300 years. The moving correlation yielded a single point of maximum agreement, $r = 0.989$ (inset), fixing the beginning of the floating Cariaco Basin varve chronology at 10,490 cal yr B.P. The gray bar shows the timing of the abrupt warming at the transition from Younger Dryas (YD) to Preboreal (PB) conditions in both chronologies. The YD transition was determined by ring widths in the German pines and by gray scale in the Cariaco Basin. ^{14}C uncertainties are shown at 1σ.

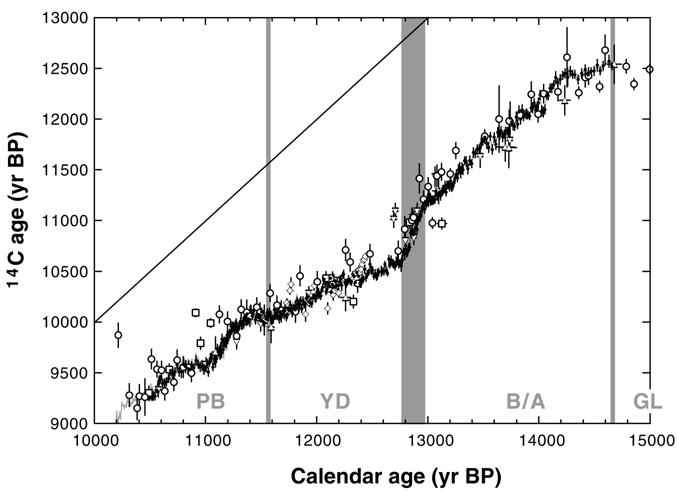

Fig. 2. Radiocarbon calibration data set from Cariaco Basin core PL07-58PC compared with those from coral U/Th dates and varved lake sediments. Thin black line and solid circles, Cariaco Basin data; thin gray line, German pine data (*1*); upright open triangles, coral U/Th from Barbados (*3*); open squares, coral U/Th from Papua New Guinea (*4*); upside-down open triangles, coral U/Th from Tahiti (*5*); open diamonds, coral U/Th from Vanuatu (*6*); and open circles, varves from Lake Suigetsu, Japan (*18*). Climatic period abbreviations are as follows: Preboreal, PB; Younger Dryas, YD; Bølling/Allerød, B/A; and Glacial, GL. Gray bars indicate timing of the Glacial-Bølling transition and the beginning and end of the Younger Dryas based on Cariaco Basin gray scale. ^{14}C and U/Th uncertainties are shown at 1σ. These data are available at (*40*) and at the NOAA NGDC World Data Center for Paleoclimatology (www.ngdc.noaa.gov/paleo/paleo.html).

Atmospheric ^{14}C concentrations calculated from 58PC calibration data reveal large variations throughout the deglacial period (Fig. 3). The most distinct features are the sharp rise and increased $\Delta^{14}C$ during the early Younger Dryas, between 13 and 11.5 cal kyr B.P. Elevated $\Delta^{14}C$ during the Younger Dryas has been reported previously (*4*, *7*, *9*, *12*), but the pattern and timing of change is revealed here in greater detail. In only 200 calendar years, $\Delta^{14}C$ rose 70 ± 10‰ (*22*), with abrupt transitions at the beginning and end of the increase. The record also shows century-scale oscillations of 20 to 30‰ occurring between 15 and 13 cal kyr B.P. A rapid rise in $\Delta^{14}C$ (25‰ in 15 years) occurs at 14.1 cal kyr B.P., followed by a brief period of elevated $\Delta^{14}C$ that lasted ~40 years before declining. More gradual $\Delta^{14}C$ increases of ~30‰ can be seen at 13.5 and 13.3 cal kyr B.P. (Fig. 3).

To facilitate comparison to other climatic and cosmogenic production records, we subtracted a linear trend from $\Delta^{14}C$ (Fig. 3). The trend is intended to represent the decline in atmospheric $\Delta^{14}C$ arising from gradually increasing geomagnetic field intensity over the interval of deglaciation (*23*). This treatment intentionally overlooks possible additional short-term (millennial-centennial) structure in some geomagnetic field strength data, which are typically within data uncertainties. The use of a simple linear model instead of a geomagnetically forced ^{14}C production model also avoids errors introduced by parameterization of uncertain long-term changes in the carbon cycle (e.g., changes in size of biosphere C reservoir). Detrended $\Delta^{14}C$ and climate proxy data from the same sediments (Fig. 4) show a significant anticorrelation ($r = -0.81$) from 15 to 12.5 cal kyr B.P. and allow precise determination of the relative timing of abrupt changes in $\Delta^{14}C$ versus climate. The timing of the $\Delta^{14}C$ rise at 13.0 cal kyr B.P. can be identified within the resolution of the sampling (± 10 years) as precisely synchronous with climatic changes during the onset of the Younger Dryas. Immediately after the Younger Dryas onset, $\Delta^{14}C$ decreases and continues to decline throughout the Younger Dryas period. At the Younger Dryas termination, $\Delta^{14}C$ shows an abrupt 25 to 30‰ drop with a distinctly different slope than the overall decline within the Younger Dryas (Fig. 4). In addition to large changes during the Younger Dryas, there is evidence for $\Delta^{14}C$ shifts concurrent with century-scale climate events as well. The sharp 25‰ $\Delta^{14}C$ increase at 14.1 cal kyr B.P. occurs precisely at the beginning of the Older Dryas cold event. In addition, a 20 to 25‰ $\Delta^{14}C$ rise is discernable at the beginning of the cold event around 13.7 cal kyr B.P. A 20‰ $\Delta^{14}C$ increase also occurs at the onset of the Inter-Allerød Cold Period around 13.3 cal kyr B.P., but this rise is more gradual and cannot be distinguished within errors from a general increase beginning earlier.

The correspondence of $\Delta^{14}C$ and climate variations suggests that both have been influenced by a common forcing mechanism (*24*). The two most plausible candidate forcings are large-scale changes in ocean circulation and variations in solar irradiance. Changes in the large-scale overturning circulation of the ocean and in the rate of formation of North Atlantic Deep Water (NADW) in particular influence the global distribution of heat and moisture as well as the sequestration of ^{14}C into the ocean interior. Different modes of thermohaline circulation have been invoked previously as a potential explanation for rapid changes in climate (*8*, *25–27*) as well as atmospheric $\Delta^{14}C$ (*4*, *7–11*). Direct evidence for ocean circulation change, including Cd/Ca and stable isotopes ($\delta^{13}C$ and $\delta^{18}O$) in benthic foraminifera from the North Atlantic Ocean, indicates that NADW formation was reduced or absent during the Younger Dryas (*25–27*). Calculations using a geochemical box-model show that the magnitude of atmospheric $\Delta^{14}C$ increase after a complete NADW shutdown may reach 80‰ (*7*). Simulations of reduced NADW formation with the use of more complex numerical and general circulation models (GCMs) result in smaller magnitude $\Delta^{14}C$ responses of 15 to 30‰, although including the effects of sea ice may roughly double the atmospheric $\Delta^{14}C$ response (*10*, *11*, *28*).

Changes in solar irradiance may also have a direct affect on climate, and associated heliomagnetic changes modulate the production of cosmogenic isotopes. Comparisons of global and Northern Hemisphere average temperature and solar irradiance trends over the past 500 years suggest that much of the preindustrial natural temperature variability may have been caused by the sun (*29*). In addition, evidence for a solar influence on $\Delta^{14}C$ is well documented by records showing $\Delta^{14}C$ increases during known periods of reduced solar activity such as the Maunder Minimum (*30*), during which irradiance is estimated to have been 0.25% lower than present (*29*). However, the largest Holocene $\Delta^{14}C$ anomalies attributed to solar forcing are only ~25 to 30‰, much smaller than the 70‰ Younger Dryas event. Also, it is unlikely that solar forcing alone produced the largest of the observed deglacial climate changes, as much as 20°C in the northern North Atlantic region. For example, GCM simulations specifying a 0.25% reduction in solar irradiance only produced

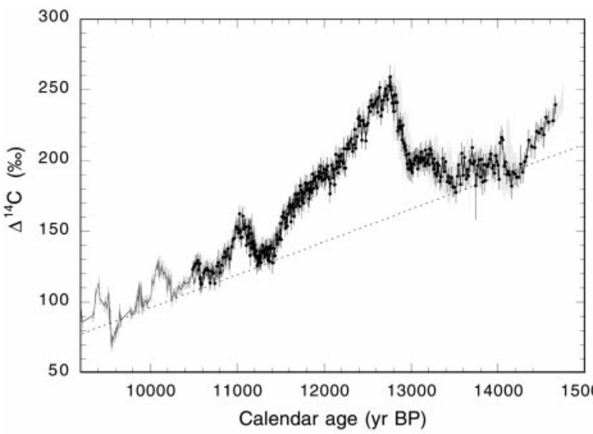

Fig. 3. Atmospheric radiocarbon concentration ($\Delta^{14}C$) calculated from Cariaco Basin and tree ring data sets. Solid circles and thin black line, Cariaco Basin core PL07-58PC data; thick gray line, German pine data (*1*) spliced to the end of the INTCAL98 data set (*2*). Dashed line is a linear model approximating geomagnetic field intensity used to detrend the raw Cariaco Basin $\Delta^{14}C$ data for comparison to other cosmogenic and paleoclimatic data sets. Error bars are 1σ uncertainty calculated by taking into account ^{14}C uncertainties only. The wide gray swath shows total $\Delta^{14}C$ uncertainty, including the uncertainty contributed by calendar age error (*22*).

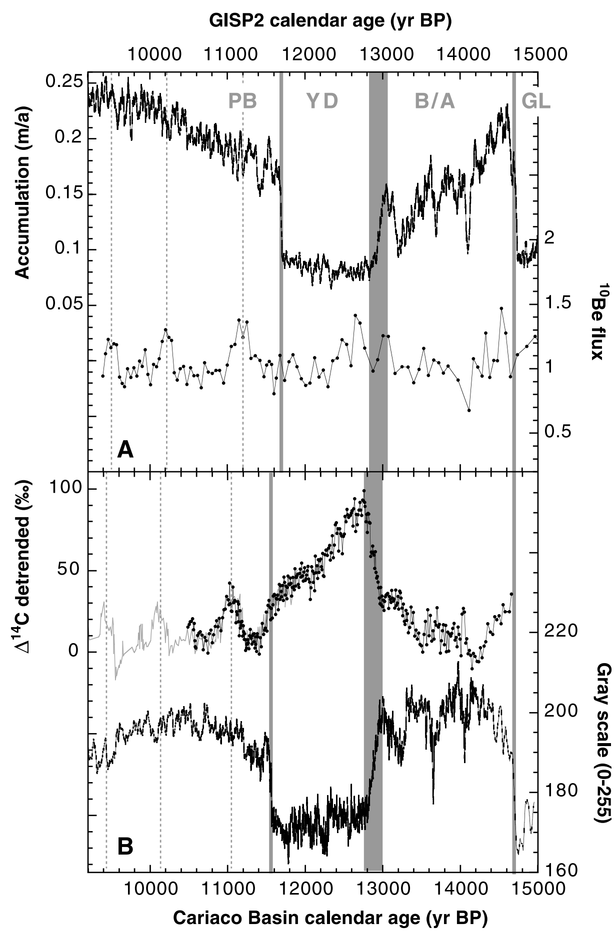

Fig. 4. Observed paleoclimate and detrended $\Delta^{14}C$ from the Cariaco Basin and tree rings compared with paleoclimate and cosmogenic isotopes from the GISP2 ice core. Each set of records during deglaciation was measured on the same core and is shown plotted on its own independent time scale, ice-layer chronology for GISP2, and anchored varve chronology for the Cariaco Basin. (**A**) Thin line (upper curve) is GISP2 ice accumulation data (*41*). Line with solid circles (lower curve) is atmospheric ^{10}Be concentration ($^{10}Be_{atm}$) calculated from ice ^{10}Be concentrations and snow accumulation measured in the GISP2 ice core (*33–35*). Gray bars indicate climate transitions based on shifts in accumulation rate. (**B**) Gray line, detrended atmospheric $\Delta^{14}C$ data from German pines (*1*) spliced together with INTCAL98 data (*2*); black line with solid circles, detrended $\Delta^{14}C$ measured in Cariaco Basin core PL07-58PC (upper curves). Black line (lower curve) is Cariaco Basin gray scale. Gray bars indicate climate transitions based on shifts in gray scale and light laminae thickness. Previous work (*7*, *14*) suggests that abrupt climate shifts in both regions were synchronous. The age differences for the events shown here (gray bars) are well within the combined errors of the Cariaco Basin and GISP2 chronologies. Dashed lines indicate century-scale anomalies common to both cosmogenic ^{10}Be and ^{14}C, seen throughout the Holocene and attributed to solar variability (*33*).

0.5° to 1.0°C surface temperature change in the same region (*31*). Thus, solar changes would have to have been at least an order of magnitude larger than those during the Maunder Minimum in order to account for observed deglacial climate changes. Although there are suggestions of possible indirect links (and amplifying mechanisms) between solar variability and climate (*32*), these remain unproven.

Direct evaluation of solar change during the Younger Dryas can be sought by comparing cosmogenic isotope records. Estimates of ^{14}C and atmospheric ^{10}Be concentration ($^{10}Be_{atm}$), derived from measurements in ice cores, covary during much of the Holocene (*33*, *34*). However, the Younger Dryas $\Delta^{14}C$ anomaly, which is by far the largest of the last 15,000 years, is not matched in amplitude by corresponding atmospheric ^{10}Be concentration estimates (Fig. 4). Thus, available ^{10}Be data do not support the interpretation of the Younger Dryas $\Delta^{14}C$ anomaly as solely or mostly due to increased production. However, it must be pointed out that the calculation of $^{10}Be_{atm}$ from ice core concentrations depends heavily on knowledge of the mode of ^{10}Be deposition, which itself may vary with changing climate (*34*, *35*). Thus, the GISP2 $^{10}Be_{atm}$ reconstruction is especially suspect before about 11.5 cal kyr B.P. and does not conclusively represent solar variability.

We conclude that the largest of the concurrent changes in climate and atmospheric $\Delta^{14}C$ during deglaciation were predominantly of ocean origin, although we cannot eliminate the possibility that some of these events were triggered by the sun. New data here allow for little or no time lag between the initial rise in $\Delta^{14}C$ and the associated Younger Dryas climate reversal. Thus, if solar changes triggered the event, the data require extremely tight coupling between solar cooling and the amplifying ocean circulation change that accounts for much or most of the observed ^{14}C and climate change. Lastly, accurate conversion of ^{14}C ages to calendrical time is essential to attempts to evaluate the behavior of the climate system from geologic data. Results presented here provide a ^{14}C calibration that spans the climatically unstable deglacial interval with resolution comparable to that previously available only from tree rings.

References and Notes

1. B. Kromer, M. Spurk, *Radiocarbon* **40**, 1117 (1998).
2. M. Stuiver *et al.*, *Radiocarbon* **40**, 1041 (1998).
3. E. Bard, M. Arnold, R. G. Fairbanks, B. Hamelin, *Radiocarbon* **35**, 191 (1993).
4. R. L. Edwards *et al.*, *Science* **260**, 962 (1993).
5. E. Bard *et al.*, *Nature* **382**, 241 (1996).
6. G. S. Burr *et al.*, *Radiocarbon* **40**, 1093 (1998).
7. K. A. Hughen *et al.*, *Nature* **391**, 65 (1998).
8. W. S. Broecker, G. H. Denton, *Geochim. Cosmochim. Acta* **53**, 2465 (1989).
9. S. Björck *et al.*, *Science* **274**, 1155 (1996).
10. T. F. Stocker, D. G. Wright, *Paleoceanography* **11**, 773 (1996).
11. U. Mikolajewicz, *Tech. Rep. 189* (Max-Planck-Inst. Für Meteorologie, Hamburg, 1996).
12. T. Goslar, M. Arnold, N. Tisnerat-Laborde, J. Czernik, K. Wieckowski, *Nature* **403**, 877 (2000).
13. L. C. Peterson, J. T. Overpeck, N. G. Kipp, J. Imbrie, *Paleoceanography* **6**, 99 (1991).
14. K. A. Hughen, J. T. Overpeck, L. C. Peterson, S. Trumbore, *Nature* **380**, 51 (1996).
15. D. E. Black *et al.*, *Science* **286**, 1709 (1999).
16. A. Shiller, U. Mikolajewicz, R. Voss, *Clim. Dyn.* **13**, 325 (1997).
17. K. J. Holman, C. G. H. Rooth, *Deep-Sea Res.* **37**, 203 (1990).
18. H. Kitigawa, J. van der Plicht, *Science* **279**, 1187 (1998).
19. The rapid shift from intense to reduced upwelling in the Cariaco Basin at the Younger Dryas–Preboreal transition is an ideal test for changes in reservoir age from local upwelling. The ^{14}C data sets show close agreement immediately before and after the rapid shift in Cariaco Basin upwelling at the Younger Dryas termination (Fig. 1). The lack of a step-wise decrease in Cariaco ^{14}C age across this boundary relative to tree rings further confirms that the Cariaco Basin reservoir age has likely remained unchanged despite variable upwelling within the basin.
20. The floating German pine chronology was itself anchored to the absolute oak dendrochrology primarily through wiggle-matching ^{14}C variations, but also through matching ring-width patterns. Uncertainty in the absolute pine age is reported conservatively at ±20 years to account for the relatively short period of overlap (<400 years), unequal spacing of ^{14}C dates, and potential missing rings (*1*). The Cariaco-pine overlap is 1370 years, and the high resolution of the two records provides a unique time lag of maximum correlation, rather than a range of lags with equally high correlation values. Due to the 10-year sampling resolution of both chronologies, we estimate an uncertainty of ±10 years in the wiggle match for a total Cariaco Basin uncertainty in the anchoring of ±30 years.
21. This marine calibration data set assumes a constant reservoir age through time. Although Cariaco reservoir age is likely unaffected by local upwelling, changes in surface Atlantic reservoir age before the overlap with tree rings may have introduced gradual shifts in Cariaco Basin reservoir age. Close agreement between (constant reservoir-corrected) Cariaco Basin and terrestrial ^{14}C data from Lake Suigetsu, however (Fig. 2), suggest that any potential shifts in reservoir age were not likely to have exceeded ±100 years. Greater certainty requires a higher-resolution terrestrial ^{14}C calibration record for the deglacial period.
22. Error bars for $\Delta^{14}C$ in Fig. 3 do not include calendar age uncertainty. Although there is uncertainty in Cariaco Basin calendar age based on uncertainty in the wiggle match to tree rings, this will affect the floating Cariaco Basin calendar chronology as a whole. Similarly, cumulative errors in counting the varve chronology will affect most adjacent points in the chronology together. Including calendar age uncertainty in the calculation of $\Delta^{14}C$ uncertainties for individual points thus would overrepresent the sample-to-sample uncertainty. Rather, the entire curve must be shifted along lines of equal ^{14}C age within a range of ±30 to 95 cal years and ±1.5 to 7‰ additional $\Delta^{14}C$ uncertainty (gray swath, Fig. 3). A similar gray swath shows total $\Delta^{14}C$ uncertainty for German pines, including calendar-age uncertainty from the pine-oak wiggle match.
23. E. Tric *et al.*, *J. Geophys. Res.* **97**, 9337 (1992).
24. Although we focus here on abrupt changes, the drawdown of $\Delta^{14}C$ during the Younger Dryas is also a large signal. Previously, we had hypothesized that increased North Atlantic Intermediate Water (NAIW, or "upper NADW") formation could explain the $\Delta^{14}C$ drawdown (*7*). Ocean GCM simulations of upper and lower NADW formation show that the shallower mode causes much less surface air warming (*36*) and could potentially draw down $\Delta^{14}C$ while not substantially influencing North Atlantic temperatures. Although increased convection in the Southern Ocean could also explain at least some of the Younger Dryas $\Delta^{14}C$ decline (*37*), Southern Ocean surface water is less well equilibrated to atmospheric CO_2 than the North Atlantic and has less leverage to draw down atmospheric $\Delta^{14}C$ (*7*). In addition, recent model simulations of ^{14}C production rate inferred from ^{10}Be records (*12*, *38*) suggest that production declined during the Younger Dryas and may have contributed to the observed drawdown as well. It is difficult at present to identify a specific cause for the Younger Dryas $\Delta^{14}C$ decline, and it is possible that it resulted from a combination of factors.
25. E. A. Boyle, L. D. Keigwin, *Nature* **330**, 35 (1987).
26. L. D. Keigwin, G. A. Jones, S. J. Lehman, E. A. Boyle, *J. Geophys. Res.* **96**, 16811 (1991).
27. T. M. Marchitto, W. B. Curry, D. W. Oppo, *Nature* **393**, 557 (1998).
28. The smaller $\Delta^{14}C$ increase simulated by ocean GCMs is primarily due to a large increase in Antarctic Bottom Water (AABW) formation compensating the reduction in NADW, whereas the box-model simulations resulting in a higher atmospheric $\Delta^{14}C$ response prescribed a smaller increase in the rate of AABW formation. It is possible that ocean GCMs do not capture fully the complex behavior of global deep ocean ventilation (i.e., overestimating the rate of Southern Ocean convection) and may therefore underestimate the atmospheric $\Delta^{14}C$ response to changes in NADW formation by as much as half.
29. J. Lean, J. Beer, R. S. Bradley, *Geophys. Res. Lett.* **22**, 3195 (1995).
30. M. Stuiver, T. F. Braziunas, B. Becker, B. Kromer, *Quat. Res.* **35**, 1 (1991).
31. D. Rind, J. T. Overpeck, *Quat. Sci. Rev.* **12**, 357 (1993).
32. B. A. Tinsley, G. W. Deen, *J. Geophys. Res.* **96**, 22283 (1991).
33. R. C. Finkel, K. Nishizumi, *J. Geophys. Res.* **102**, 26699 (1997).
34. R. B. Alley *et al.*, *J. Glaciol.* **41**, 503 (1995).
35. ^{10}Be can be deposited directly onto the ice sheet (dry) or scoured from the air by falling snowflakes (wet). The mode of deposition dictates how ^{10}Be concentration in ice will be corrected for changes in ice accumulation rate in order to derive $^{10}Be_{atm}$. A linear, empirical relation was measured between ^{10}Be flux and snow flux for the Holocene, effectively assuming a constant ratio of wet and dry ^{10}Be deposition (a reasonable assumption for the stable climate of the Holocene). The same relation was then used to calculate $^{10}Be_{atm}$ back through the deglacial and glacial periods. Unfortunately, there is little evidence to support the assumption that modes of ^{10}Be deposition did not change with climate, and the record of $^{10}Be_{atm}$ during deglaciation must be considered equivocal.
36. S. Rahmstorf, *Nature* **372**, 82 (1994).
37. W. S. Broecker, *Paleoceanography* **13**, 119 (1998).
38. O. Marchal, T. F. Stocker, R. Muscheler, *Earth Plan. Sci. Lett.*, in preparation; O. Marchal, personal communication.
39. M. Friedrich, B. Kromer, M. Spurk, J. Hofmann, K. F. Kaiser, *Quat. Internat.* **61**, 27 (1999).
40. Web table 1 is available at *Science* Online at www.sciencemag.org/cgi/content/full/290/5498/1951/DC1.
41. R. B. Alley *et al.*, *Nature* **362**, 527 (1993).

42. We thank two anonymous reviewers for comments that helped improve the manuscript. Supported by NSF Earth Systems History (ESH) grant No. ATM-9709563, and by a NOAA Climate and Global Change postdoctoral fellowship to K.A.H., as well as by the Department of Energy through Lawrence Livermore National Laboratory under contract No. W-7405-Eng-48. We are especially grateful for the tireless work of C. Herring, without whose efforts this research would not have been completed.

15 September 2000; accepted 31 October 2000